
Keep Various Trajectories: Promoting Exploration of Ensemble Policies in Continuous Control

Chao Li^{1,4} Chen Gong² Qiang He³ Xinwen Hou^{1†}

¹Institute of Automation, Chinese Academy of Sciences, China

²University of Virginia, USA

³University of Tübingen, Germany

⁴University of Chinese Academy of Sciences, China

{lichao2021, xinwen.hou}@ia.ac.cn

fzv6en@virginia.edu, qianghe97@gmail.com

Abstract

The combination of deep reinforcement learning (DRL) with ensemble methods has been proved to be highly effective in addressing complex sequential decision-making problems. This success can be primarily attributed to the utilization of multiple models, which enhances both the robustness of the policy and the accuracy of value function estimation. However, there has been limited analysis of the empirical success of current ensemble RL methods thus far. Our new analysis reveals that the sample efficiency of previous ensemble DRL algorithms may be limited by sub-policies that are not as diverse as they could be. Motivated by these findings, our study introduces a new ensemble RL algorithm, termed **Trajectories-awarE Ensemble exploratioN** (TEEN). The primary goal of TEEN is to maximize the expected return while promoting more diverse trajectories. Through extensive experiments, we demonstrate that TEEN not only enhances the sample diversity of the ensemble policy compared to using sub-policies alone but also improves the performance over ensemble RL algorithms. On average, TEEN outperforms the baseline ensemble DRL algorithms by 41% in performance on the tested representative environments.

1 Introduction

Deep Reinforcement Learning (DRL) [1] has demonstrated significant potential in addressing a range of complex sequential decision-making problems, such as video games [2; 3; 4], autonomous driving [5; 6], robotic control tasks [7; 8], board games [9; 10], etc. Although the combination of high-capacity function approximators, such as deep neural networks (DNNs), enables DRL to solve more complex tasks, two notorious problems impede the widespread use of these DRL in real-world domains. i) *function approximation error*: Q-learning algorithm converges to sub-optimal solutions due to the error propagation [11; 12; 13], e.g., the maximization of random function approximation errors accumulate into consistent overestimation bias [14]. ii) *sample inefficiency*, model-free algorithm is notorious for requiring sample diversity—training of neural networks requires a large number of samples which is hard to acquire in real-world scenarios.

Ensemble reinforcement learning shows great potential in solving the issues mentioned above by combining multiple models of the value function and (or) policy [14; 15; 16; 17; 18; 19; 20] to improve the accuracy and diversity. For instance, Max-Min Q-learning [11] reduces estimation bias by utilizing an ensemble of estimates and selecting the minimum value as the target estimate. Bootstrapped DQN [15] and SUNRISE [16] train an ensemble of value functions and policies,

[†]Corresponding Author.

leveraging the uncertainty estimates of value functions to enrich the diversity of learning experiences. However, we claim that existing ensemble methods do not effectively address the crucial issue of diverse exploration, which is essential for enhancing sample efficiency. Although randomly initializing sub-policies shares some similarities to adding random noise with the ensemble policy, it is not sufficient for significantly improving the sample diversity of the ensemble policy. Thus, how to enhance the exploration diversity of ensemble policy remains an open question.

This paper presents a novel approach called **Trajectories-awarE Ensemble exploratioN** (TEEN) that encourages diverse exploration of ensemble policy by encouraging diverse behaviors through exploration of the state-action visit distribution measure space. The state-action visit distribution measure quantifies the frequency with which a particular state-action pair is visited when using a certain policy. Thus, policies with diverse state-action visit distributions induce different trajectories [21]. Moreover, value functions are learned from the trajectories generated by the policy, rather than the actions the policy may take. While previous research [22; 23; 24] has emphasized promoting diverse actions, this approach does not always lead to diverse trajectories. This paper highlights the importance of diverse trajectories in improving sample efficiency, which TEEN achieves.

Our contributions can be summarized in three aspects. (1) We propose **Trajectories-awarE Ensemble exploratioN** (TEEN) algorithm, a highly sample-efficient ensemble reinforcement learning algorithm. TEEN trains sub-policies to exhibit a greater diversity of behaviors, accomplished by considering the distribution of trajectories. (2) Theoretical analysis confirms that our algorithm facilitates more diverse exploration by enhancing the varied behaviors of the sub-policies. (3) Extensive experimental results show that our method outperforms or achieves a similar level of performance as the current state-of-the-art across multiple environments, which include both MuJoCo control [25] tasks and DMControl tasks [26]. Specifically, on average across the tasks we investigated, TEEN surpasses the baseline ensemble DRL algorithm by 41% and the state-of-the-art off-policy DRL algorithms by 7.3% in terms of performance. Furthermore, additional experiments demonstrate that our algorithm samples from a diverse array of trajectories.

2 Related Work

Ensemble Methods. Ensemble methods have been widely utilized in DRL to serve unique purposes. Overestimation bias in value function severely undermines the performance of Q-learning algorithms, and a variety of research endeavors on the ensemble method have been undertaken to alleviate this issue [14; 18; 19; 27; 11; 28]. TD3 [14] clips Double Q-learning to control the overestimation bias, which significantly improves the performance of DDPG [29]. Maxmin Q-learning [11] directly mitigates the overestimation bias by using a minimization over multiple action-value estimates. Ensemble methods also play a role in encouraging sample efficient exploration [30]. For example, Bootstrapped DQN [15] leverages uncertainty estimates for efficient (and deep) exploration. On top of that, REDQ [17] enhances the sample efficiency by using a update-to-data ratio $\gg 1$. SUNRISE [16] turns to an ensemble policy to consider for compelling exploration.

Diverse Policy. A range of works have been proposed for diverse policy, and these can generally be classified into three categories [31]. The first category involves directly optimizing policy diversity during pre-training without extrinsic rewards. Fine-tuning with rewards is then applied to complete the downstream tasks. These methods [32; 33; 34; 35] train the policy by maximizing the mutual information between the latent variable and the trajectories, resulting in multiple policies with diverse trajectories. The second category addresses constraint optimization problems, where either diversity is optimized subject to quality constraints, or the reverse is applied – quality is optimized subject to diversity constraints [36; 37; 38; 39]. The third category comprises quality diversity methods [31; 40; 41], which prioritize task-specific diversity instead of task-agnostic diversity. These methods utilize scalar functions related to trajectories and simultaneously optimize both quality and diversity.

Efficient Exploration. Efficient exploration methods share similar methods to diverse policy methods in training the agent, wherein exploration by diverse policies can enhance the diversity of experiences, ultimately promoting more efficient exploration. [42]. Other prior works focusing on efficient exploration consider diverse explorations within a single policy, with entropy-based methods being the representative approach [22; 43]. These methods strive to simultaneously maximize the expected cumulative reward and the entropy of the policy, thus facilitating diverse exploration. Additionally,

another representative category of research is the curiosity-driven method [24; 23; 44]. These methods encourage the agent to curiously explore the environment by quantifying the state with "novelty", such as state visit counts [23], model prediction error [24], etc.

3 Preliminaries

3.1 Markov Decision Process

Markov Decision Process (MDP) can be described as a tuple $\langle \mathcal{S}, \mathcal{A}, P, r, \gamma \rangle$, where \mathcal{S} and \mathcal{A} represent the state and action spaces, respectively. The function P maps a state-action pair to the next state with a transition probability in the range $[0, 1]$, i.e., $P : \mathcal{S} \times \mathcal{A} \times \mathcal{S} \rightarrow [0, 1]$. The reward function $r : \mathcal{S} \times \mathcal{A} \rightarrow \mathbb{R}$ denotes the reward obtained by performing an action a in a particular state s . Additionally, $\gamma \in (0, 1)$ is the discount factor. The goal of reinforcement learning algorithms is to find a policy π^* that maximizes the discounted accumulated reward $J(\pi)$, defined as:

$$J(\pi) = \mathbb{E}_{s, a \sim \pi} [\sum_{t=0}^{\infty} \gamma^t r(s_t, a_t)] \quad (1)$$

3.2 Overestimation Bias in Deep Deterministic Policy Gradient

The Deep Deterministic Policy Gradient (DDPG) algorithm [45; 29] forms the foundation of various continuous control tasks such as TD3 [14] and SAC [22]. By enabling policy output to produce deterministic actions, DDPG offers a powerful algorithmic solution to these tasks. DDPG utilizes two neural networks: the actor and critic networks. The actor network is responsible for generating the policy, while the critic network evaluates the value function. In deep reinforcement learning (DRL), the policy $\pi(a|s)$ and the value function $Q(s, a)$ are expressed by deep neural networks parameterized with ϕ and θ respectively. DDPG suggests updating the policy through a deterministic policy gradient, as follows:

$$\nabla_{\phi} J(\phi) = \mathbb{E}_{s \sim P_{\pi}} [\nabla_a Q^{\pi}(s, a)|_{a=\pi(s)} \nabla_{\phi} \pi_{\phi}(s)] \quad (2)$$

In order to approximate the discounted cumulative reward (as specified in Eq.(1)), the function $Q(s, a)$ is updated by minimizing the temporal difference (TD) errors [46] between the estimated value of the next state s' and the current state s .

$$\theta^* = \arg \min_{\theta} \mathbb{E} [r(s, a) + \gamma Q_{\theta}^{\pi}(s', a') - Q_{\theta}^{\pi}(s, a)]^2 \quad (3)$$

In policy evaluation, Q function is used to approximate the value by taking action a in state s . The Q function is updated by Bellman equation [47] with bootstrapping, where we minimize the expected Temporal-Difference (TD) [46] error $\delta(s, a)$ between value and the target estimate in a mini-batch of samples \mathcal{B} ,

$$\delta(s, a) = \mathbb{E}_{\mathcal{B}} [r(s, a) + \max_{a'} Q(s', a') - Q(s, a)] \quad (4)$$

This process can lead to a consistent overestimation bias as the holding of Jensen's inequality [48]. Specifically, the overestimation of value evaluation arises due to the following process:

$$\mathbb{E}_{\mathcal{B}} [\max_{a' \in \mathcal{A}} Q(s', a')] \geq \max_{a' \in \mathcal{A}} \mathbb{E}_{\mathcal{B}} [Q(s', a')] \quad (5)$$

4 Methodology

This section describes Trajectories-awarE Ensemble exploratioN (TEEN) method that achieves diverse exploration for agents. TEEN aims to enforce efficient exploration by encouraging diverse behaviors of an ensemble of N sub-policies parameterized by $\{\phi_i\}_{i=1}^N$. TEEN initially formulates a discrepancy measure and enforces the discrepancy among the sub-policies while simultaneously maximizing the expected return. Next, we present how to solve this optimization problem indirectly by utilizing the mutual information theory. Finally, we conduct a theoretical analysis to ensure whether the diversity of the samples collected by the ensemble policy is enhanced by solving this optimization problem. We summarize TEEN in Algorithm 1.

4.1 Discrepancy Measure

We assess the diverse behaviors of policies by examining the diversity of trajectories generated by their interactions with the environments. The state-action visit distribution, indicating the probability of encountering a specific state-action pair when initiating the policy from a starting state, encapsulates the diversity of these trajectories directly. Thus, TEEN measures the diverse behaviors of policies by directly assessing their state-action visit distribution. Formally, given an ensemble of N sub-policies $\{\pi_0, \pi_1, \dots, \pi_k, \dots, \pi_N\}$, we use ρ^{π_k} to induce the state-action visit distribution deduced by policy π_k and use ρ for the ensemble policy. We have,

$$\rho = \frac{1}{N} \sum_{k=1}^N \rho^{\pi_k} \quad (6)$$

For convenience, we use the conditioned state-action visit probability, denoted as $\rho(s, a|z)$, to represent the respective state-action visit distribution of each sub-policy. This can be expressed as follows,

$$\rho^{\pi_k}(s, a) = \rho(s, a|z_k) \quad (7)$$

Where $\{z_k\}^N$ is the latent variable representing each policy. Our discrepancy measure \mathcal{KL} -divergence is an asymmetric measure of the difference between two probability distributions. Given this discrepancy measure, we define the difference of policies as the \mathcal{KL} -divergence of the conditioned state-action visit distribution with the state-action visit distribution.

Definition 1 (Difference between Policies) Given an ensemble of N policies $\{\pi_0, \pi_1, \dots, \pi_k, \dots, \pi_N\}$, the difference between policy π_k and other policies can be defined by the conditioned state-action occupation discrepancy:

$$\mathcal{D}_{\mathcal{KL}}[\rho^{\pi_k} || \rho] := \mathcal{D}_{\mathcal{KL}}[\rho(s, a|z_k) || \rho(s, a)] \quad (8)$$

Consequently, we improve the difference between the conditioned state-action visit distribution to enforce diverse behaviors of sub-polices. While directly optimizing the Eq. (8) can be hard: Obtaining the state-action visit distribution can be quite challenging. In response to this, Liu, H., et al., as referenced in citation [49], have suggested the use of K-Nearest Neighbors (KNN) as an approximate measure for this distribution. We notice that it can be expressed by the form of entropy discrepancy:

$$\mathbb{E}_z [\mathcal{D}_{\mathcal{KL}}(\rho(s, a|z) || \rho(s, a))] = \mathcal{H}(\rho) - \mathcal{H}(\rho|z) \quad (9)$$

In which the $\mathcal{H}[\cdot]$ is the Shannon Entropy with base e , $\mathcal{H}(\rho)$ is the entropy of the state-action visit distribution. With the mutual information theory, we can transform this optimization target as follows:

$$\mathcal{H}(\rho) - \mathcal{H}(\rho|z) = \mathcal{H}(z) - \mathcal{H}(z|\rho) \quad (10)$$

Thus, we turn to this equivalent optimization target. The first term encourages a high entropy of $p(z)$. We fix $p(z)$ to be uniform in this approach by randomly selecting one of the sub-policies to explore. We have $\mathcal{H}(z) = -\frac{1}{N} \sum_{k=1}^N \log p(z_k) \approx \log N$, which is a constant. The second term emphasises the sub-policy is easy to infer given a state-action pair. We approximate this posterior with a learned discriminator $q_\zeta(z|s, a)$ and optimize the variation lower bound.

$$\begin{aligned} \mathcal{H}(z) - \mathcal{H}(z|\rho) &= \log N + \mathbb{E}_{s, a, z} [\log \rho(z|s, a)] \\ &= \log N + \mathbb{E}_{s, a} [\mathcal{D}_{\mathcal{KL}}(\rho(z|s, a) || q_\zeta(z|s, a))] + \mathbb{E}_{s, a, z} [\log q_\zeta(z|s, a)] \\ &\geq \log N + \mathbb{E}_{s, a, z} [\log q_\zeta(z|s, a)] \end{aligned} \quad (11)$$

Where we use non-negativity of KL-divergence, that is $\mathcal{D}_{\mathcal{KL}} \geq 0$. We minimize $\mathcal{D}_{\mathcal{KL}}[\rho(z|s, a) || q_\zeta(z|s, a)]$ with respect to parameter ζ to tighten the variation lower bound:

$$\nabla_\zeta \mathbb{E}_{s, a} [\mathcal{D}_{\mathcal{KL}}(\rho(z|s, a) || q_\zeta(z|s, a))] = -\mathbb{E}_{s, a} [\nabla_\zeta \log q_\zeta(z|s, a)] \quad (12)$$

Consequently, we have the equivalent policy gradient with regularizer:

$$\pi^* = \arg \max_{\pi \in \Pi} J(\pi) + \alpha \mathbb{E}_{(s, a, z) \sim \rho} [\log q_\zeta(z|s, a)] \quad (13)$$

4.2 Trajectories-aware Ensemble Exploration

We select TD3 [14] as the algorithm of sub-policies which is not a powerful exploration algorithm. We then show how to ensemble algorithm with poor exploration performance and encourage efficient ensemble exploration by solving this optimization problem. We consider an ensemble of N TD3 agents i.e., $\{Q_{\theta_k}, \pi_{\phi_k}\}_{k=1}^N$, where θ_k and ϕ_k denote the parameters of k -th Q-function and sub-policy. Combined with deterministic policy gradient method [29], we update the each sub-policy by policy gradient with regularizer.

$$\nabla J_{total}(\phi_k) = \mathbb{E}_{s \sim \rho} [\nabla_a (Q^\pi(s, a) + \alpha \log q_\zeta(z_k | s, a))|_{a=\pi_{\phi_k}(s)} \nabla_{\phi_k} \pi_{\phi_k}(s)] \quad (14)$$

Recurrent Optimization. Updating all sub-policies every time step in parallel may suffer from the exploration degradation problem [35]. Consider a state-action pair (s, a_1) , which is frequently visited by sub-policy π_k and another state-action pair (s, a_2) which is visited by multiple sub-policies such that we have $q_\zeta(z_k | s, a_1) > q_\zeta(z_k | s, a_2)$. Under this circumstance, the constraint encourage sub-policy π_k to execute action a_1 while preventing from executing action a_2 which leads to the problem that some explored state-actions are prevented from being visited by the sub-policies. To tackle this challenge, we employ a recurrent training method for our sub-policies. In particular, given an ensemble of N sub-policies, we randomly select a single sub-policy, denoted as π_k , every T episodes. We then concentrate our efforts on regulating the behavior of the selected sub-policy, rather than all sub-policies simultaneously.

Gradient Clip. TEEN uses $\alpha \mathbb{E}_{(s, a, z) \sim \rho} [\log q_\zeta(z | s, a)]$ as a constraint to optimize the policy, while the gradient of this term is extremely large when the probability $q_\zeta(z | s, a)$ is small. And a state-action with small probability to infer the corresponding sub-policy z_k implies that the state-action is rarely visited by sub-policy z_k but frequently visited by other sub-policies. The target of the constraint is to increase the discrepancy of the sub-policies, while making the sub-policy visit this state-action will instead reduce the discrepancy. Further, for a state-action with large probability $q_\zeta(z | s, a)$, continuing to increase this probability will prevent the sub-policy from exploring other possible state-actions. Thus, we use the clipped constraint and the main objective we propose is the following:

$$\pi^* = \arg \max_{\pi \in \Pi} J(\pi) + \alpha \mathbb{E}_{s, a, z} [\log \text{clip}(q_\zeta(z | s, a), \epsilon, 1 - \epsilon)] \quad (15)$$

where ϵ is a hyper-parameter, and we set $\epsilon = 0.1$ for all of our experiments.

4.3 Controlling the Estimation Bias

In Q-value estimation, we share some similarities with Max-Min DQN [11] and Averaged DQN [50]. While Max-Min DQN takes the minimum over an ensemble of value functions as the target encouraging underestimation, Averaged DQN reduces the variance of estimates by using the mean of the previously learned Q-values. We combine these two techniques and apply both mean and min operators to reduce overestimation bias and variance. Instead of using the mean of the previously learned Q-values, we use the mean value on N actions of N sub-policies. TEEN then uses the minimum over a random subset \mathcal{M} of M Q-functions as the target estimate.

$$Q^{target} = r(s, a) + \gamma \min_{i=1, 2, \dots, M} \frac{1}{N} \sum_{j=1}^N Q_i(s, \pi_j(s)) \quad (16)$$

We give some analytical evidences from the perspective of order statistics to show how we control the estimation bias by adjusting M and N .

Theorem 1. Let X_1, X_2, \dots, X_N be an infinite sequence of i.i.d. random variables with a probability density function (PDF) of $f(x)$ and a cumulative distribution function (CDF) of $F(x)$. Denote $\mu = \mathbb{E}[X_i]$ and $\sigma^2 = \mathbb{V}[X_i]$. Let $X_{1:N} \leq X_{2:N} \leq X_{3:N} \dots \leq X_{N:N}$ be the order statistics corresponding to $\{X_i\}_N$. Denote PDF and CDF of the k -th order statistic $X_{k:N}$ as $f_{k:N}$ and $F_{k:N}$ respectively. The following statements hold.

$$(i) \mu - \frac{(N-1)\sigma}{\sqrt{2N-1}} \leq \mathbb{E}[X_{1:N}] \leq \mu, N > 1. \mathbb{E}[X_{1:N+1}] \leq \mathbb{E}[X_{1:N}]$$

Algorithm 1 Trajectories-Aware Ensemble Exploration algorithm (TEEN)

```

1: Initialize  $N$  policy parameters  $\phi_k$ ,  $N$  Q-function parameters  $\theta_k$ ,  $k = 1, 2, \dots, N$ 
2: Initialize target Q-function parameters  $\theta'_k \leftarrow \theta_k$ ,  $k = 1, 2, \dots, N$ .
3: Initialize discriminator  $q_\zeta$ 
4: Initialize empty replay buffer  $\mathcal{D}$ 
5: Initialize recurrent interval  $d$ 
6: for each iterations do
7:   Randomly sample a policy  $\pi_k$ 
8:   for each time step  $t$  do
9:     Choose one action with noise  $a_t = \pi_{\phi_k}(s) + \epsilon$ ,  $\epsilon \sim \mathcal{N}(0, \sigma)$ 
10:    Collect state  $s_{t+1}$  and reward  $r_t$  from the environment by taking action  $a_t$ 
11:    Store transition  $\tau_t = (s_t, a_t, s_{t+1}, r_t)$  in replay buffer  $\mathcal{B} \leftarrow \mathcal{B} \cup \tau_t$ 
12:   end for
13:   if  $t \bmod d$  then
14:     Randomly select one sub-policy  $\pi_{\phi_i}$ 
15:   end if
16:   for each gradient step do
17:     Sample random minibatch  $\mathcal{B} = \{\tau_t\}^B \sim \mathcal{D}$ 
18:     Randomly select a set  $\mathcal{M}$  of  $M$  distinct indices from  $\{1, 2, \dots, N\}$ .
19:     Compute the  $Q$  target  $y$  by Eq. (16)
20:     For all of the value functions, update  $\theta_k$  using gradient decent
21:

$$\nabla_{\theta_k} \frac{1}{|B|} \sum_{(s, a, r, s') \in \mathcal{B}} (y - Q_{\theta_k}(s, a))^2$$

22:     For sub-policy  $\pi_{\phi_i}$ , update  $\phi_i$  by gradient decent
23:

$$\nabla_{\phi_i} \frac{1}{|B|} \sum_{(s, a, r, s') \in \mathcal{B}} (\alpha \log q_\zeta(z_i | s, a) - Q_{\theta_i}(s, a)), \quad a = \pi_{\phi_i}(s)$$

24:     Update target Q-function by  $\theta'_k \leftarrow \rho \theta_k + (1 - \rho) \theta'_k$ 
25:     Update discriminator  $q_\zeta$  by Eq. (12)
26:   end for
27: end for

```

(ii) Let $\bar{X} = \frac{1}{N} \sum_{i=1}^N X_i$, then, $\mathbb{E}[\bar{X}] = \mu$, $Var[\bar{X}] = \frac{1}{N} \sigma^2$

Points 1 of the Theorem indicates that the minimum over an ensemble of values reduces the expected value, which implies that we can control the estimation from over estimates to under or proper estimates. The second point indicates that the mean over an ensemble of values reduces the variance. Thus, by combining these two operators, we control the estimation bias and the variance.

4.4 Theoretical Analysis

We analyze the diversity of state-actions gathered by ensemble policy on the basis of Shannon entropy $\mathcal{H}[\cdot]$, a commonly used diversity measure [32; 34; 51], which is a measure of the dispersion of a distribution. A high entropy of the state-action visit distribution implies that the trajectory distribution is more dispersed, which means more diverse trajectories. Thus, to achieve diverse trajectories, we maximize the expected return while maximizing the entropy of the state-action visit distribution:

$$\pi^* = \arg \max_{\pi \in \Pi} J(\pi) + \alpha \mathcal{H}[\rho^\pi] \quad (17)$$

Where ρ^π deduce the state-action visit distribution induced by the ensemble policy π and α is the weighting factor. The diversity of trajectories gathered by the ensemble policy comes from two

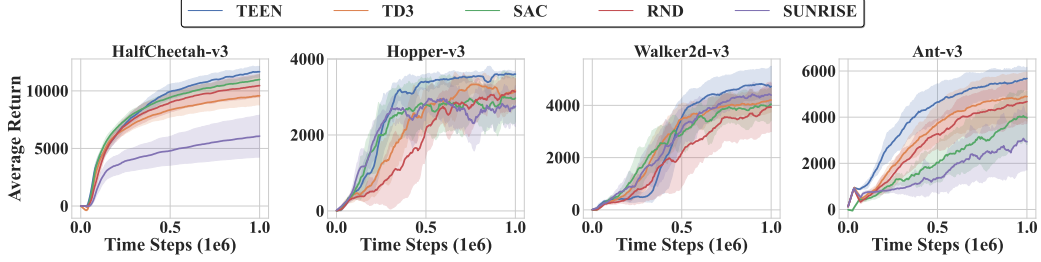


Figure 1: Learning curves for 4 MuJoCo continuous control tasks. For better visualization, the curves are smoothed uniformly. The bolded line represents the average evaluation over 10 seeds. The shaded region represents a standard deviation of the average evaluation over 10 seeds.

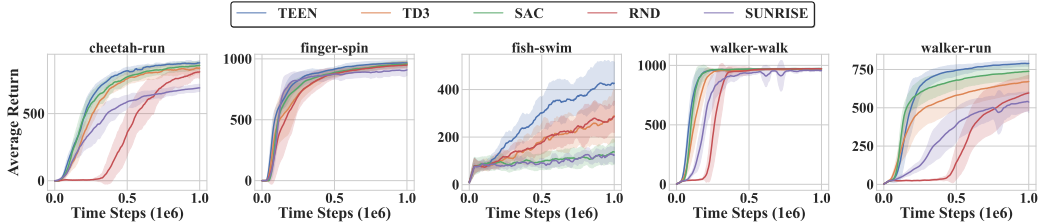


Figure 2: Learning curves for 5 continuous control tasks on DMControl suite. For better visualization, the curves are smoothed uniformly. The bolded line represents the average evaluation over 10 seeds. The shaded region represents the standard deviation of the average evaluation over 10 seeds.

components: the discrepancy of sub-policies and the diversity of trajectories gathered by the sub-policies. To illustrate that,

Lemma 1 (Ensemble Sample Diversity Decomposition) Given the state-action visit distribution of the ensemble policy ρ . The entropy of this distribution is $\mathcal{H}(\rho)$. Notice that this term can be decomposed into two parts:

$$\mathcal{H}(\rho) = \mathbb{E}_z[\mathcal{D}_{\mathcal{KL}}(\rho(s, a|z_k) || \rho(s, a))] + \mathcal{H}(\rho|z) \quad (18)$$

Where the first term is the state-action visit distribution discrepancy between the sub-policies and the ensemble policy induced by \mathcal{KL} -divergence measure. The second term implies the diversity of state-action visited by sub-policies which depends on which algorithm is used for the sub-policy, such as TD3 [14], SAC [22], RND [24], etc.

As shown in this inequality, $\mathcal{H}(\rho)$ is irrelevant of ensemble size N . Therefore, the ensemble size may improve the diversity of the ensemble policy by influencing the discrepancy of sub-policies indirectly, which implies that the diversity is not guaranteed with the increased ensemble size. Our method increases the discrepancy of sub-policies which theoretically improve the sample diversity of the ensemble policy.

5 Experimental Setup

This section presents the experimental setup used to evaluate our proposed TEEN and assesses its performance in the MuJoCo environments.

Environments. We evaluate our algorithm on several continuous control tasks from MuJoCo control suite [25] and DeepMind Control Suite [26]. We conduct experiments on 4 control tasks in MuJoCo control suite namely HalfCheetah-v3, Hopper-v3, Walker2d-v3, Ant-v3. In Halfcheetah-v3, the task is to control a cheetah with only one forefoot and one hind foot to run forward. In Hopper-v3, we control a single-legged robot to hop forward and keep balance when hopping. Walker2d-v3 is a bipedal robot environment, where we train the agent to walk or run forward. The target of Ant-v3 is to train a quadrupedal agent to stay balance and move forward. These four environments are all challenging continuous control tasks in MuJoCo. On DeepMind Control Suite, we evaluate our algorithm in 5 environments: cheetah-run, finger-spin, fish-swim, walker-walk, walker-run.

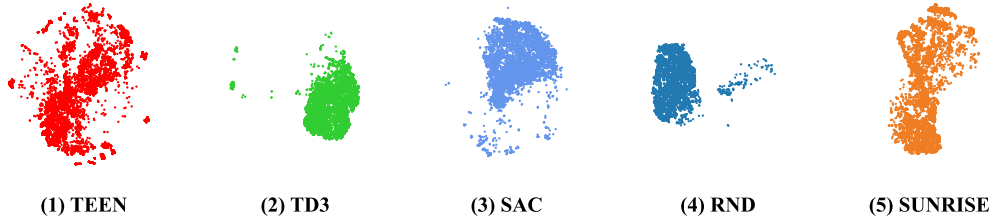


Figure 3: Measuring the exploration region. The points represent region explored by each method in 10 episodes. All the states get dimension reduction by the same t-SNE transformation for better visualization.

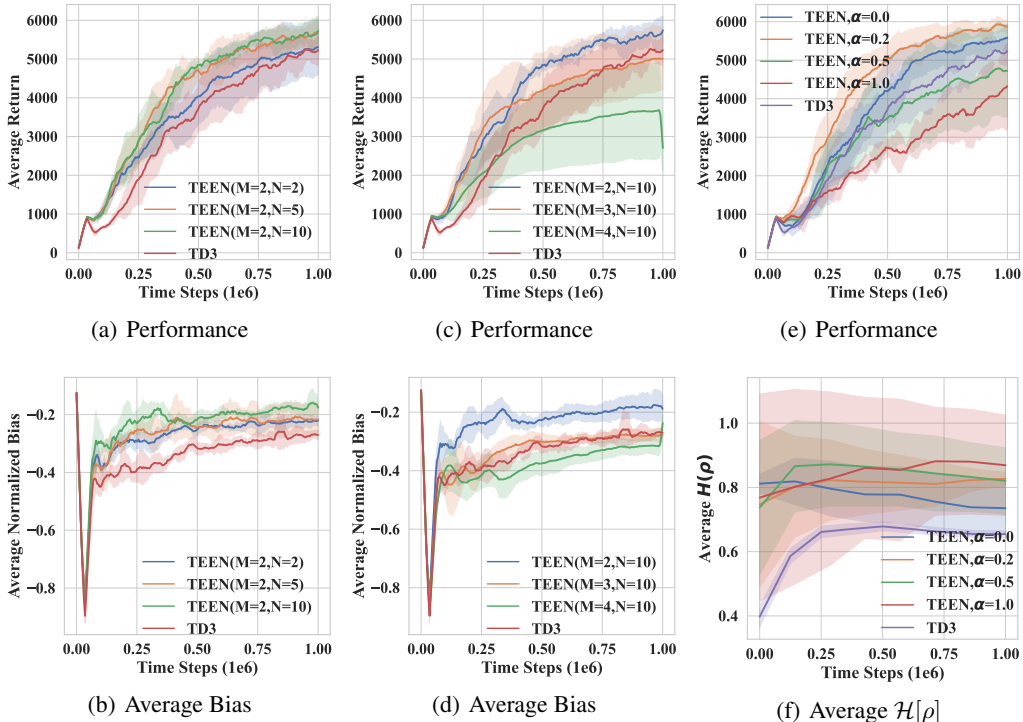


Figure 4: TEEN ablation results for Ant environment. The first column shows the effect of ensemble size N on both performance and estimation bias. The second column shows the effect of target value number M on both performance and estimation bias. The third column shows the effect of weight parameter α on both performance and the entropy of trajectories.

Baselines. Beyond simply comparing our approach with the foundational algorithm TD3 [14], a leading-edge deterministic policy gradient reinforcement learning algorithm, we also contrast our method with other efficient exploration algorithms across three distinct categories. We examine curiosity-based exploration baselines, such as RND [24], which promotes efficient exploration through intrinsic curiosity rewards. Regarding maximum entropy-based exploration, we consider SAC [22], an off-policy deep reinforcement learning algorithm that offers sample-efficient exploration by maximizing entropy during training. For ensemble exploration, we look at SUNRISE [16], a unified framework designed for ensemble-based deep reinforcement learning.

Evaluation. We follow the standard evaluation settings, carrying out experiments over one million (1e6) steps and running all baselines with ten random seeds per task to produce the main results. We maintain consistent learning rates and update ratios across all baselines. Further details regarding these parameters can be found in the Appendix B.2. For replication of TD3, SAC and SUNRISE, we use the code the author released for each baseline without any modifications to ensure the performance. For the reproduction of RND, we follow to the repository provided in the original code. For a fair

Table 1: Performance on MuJoCo Control Suite at 500K and 1M timesteps. The results show the average returns with mean and variance over 10 runs. The maximum value for each task is bolded.

500K Step	HalfCheetah	Hopper	Walker2d	Ant
TEEN	10139±623	3548±100	4034±547	5009±649
TD3	8508±601	3330±135	3798±511	4179±809
SAC	9590±419	3332±223	3781±521	3302±798
RND	9185±813	2814±536	2709±1341	3666±685
SUNRISE	4955±1249	3426±99	3782±516	1964±1020
1M Step				
TEEN	11914 ± 448	3687 ± 57	5099±513	5930 ± 486
TD3	9759±778	3479±147	4229±468	5142 ± 940
SAC	11129±420	3484±128	4349±567	5084±901
RND	10629±942	3148±143	4197±791	4990±789
SUNRISE	6269±1809	3644±75	4819±398	3523±1430

comparison, we use fully connected network with 3 layers as the architecture of the critic networks and actor networks. The learning rate for each network is set to be $3e - 4$ with Adam [52] as the optimizer. The implementation details for each baseline can be found in Appendix B.2.

6 Experimental Results

We conducted experiments to evaluate our algorithm’s performance in addressing three key research questions (RQ). Specifically, we sought to determine whether TEEN outperforms the current state-of-the-art across multiple environments and achieves a boarder range of exploration region, as well as how the ensemble size and discrepancy of sub-policies (defined in Eq. 9) impact TEEN’s performance.

RQ1: Whether TEEN outperforms the current state-of-the-art across multiple environments?
Table 1 and Table 2 report the average returns with mean and variance of evaluation roll-outs across all algorithms. The learning curves during training on MuJoCo control suite are shown in Figure 1. Learning curves for DeepMind Control suite can be found in Figure 2. On MuJoCo continuous control suite, TEEN shows superior performance across all environments which implies that by ensemble sub-policies with weak exploration performance, such as TD3, the exploration performance of the ensemble policy enhances evenly exceeding algorithms with strong exploration performance, SAC, RND, etc. While purely ensembling multiple models may not certainly improve the performance. Although SUNRISE improves the exploration performance by UCB exploration [53], it does not take effect when the uncertainty shows little relevance to the environment, and even degrades the performance (as shown in HalfCheetah-v3). TEEN can be seen as an immediate solution for diverse exploration within ensemble reinforcement learning by directly enforcing an ensemble policy to discover a broader range of trajectories. We further conduct experiments to validate that TEEN achieves a boarder exploration region (Figure 3). For a fair comparison, all the algorithms are trained in Ant-v3 with the same seed at half of the training process. In order to get reliable results, the states explored are gathered in 10 episodes with different seeds. We apply the same t-SNE transformation to the states explored by all of the algorithms for better visualization.

RQ2: How the ensemble size N and number of target values M impact TEEN’s performance?
We make experiments in Ant-v3 environment from OpenAI gym. As shown in Figure 3, when using $M = 2$ as the number of target values, the estimate of the target value is underestimated and the estimation bias increases with the increase of M . This underestimation is mitigated with an increase in ensemble size N resulting in better performance. Thus, we choose 10 to be the ensemble size for all the environments. To enhance reliability, we conducted ablation studies in various MuJoCo

Table 2: Performance on DeepMind Control Suite at 500K and 1M timesteps. The results show the average returns with mean and variance over 10 runs. The maximum value for each task is bolded.

500K Step	Cheetah-Run	Finger-Spin	Fish-Swim	Walker-Walk	Walker-Run
TEEN	837±23	928±22	381±71	970±6	754±33
TD3	784±50	891±24	260±77	968±5	592±87
SAC	791±46	897±30	155±34	972±4	688±55
RND	408±159	894±32	254±42	963±20	180±107
SUNRISE	606±37	885±38	201±34	954±16	406±99
1M Step					
TEEN	891±7	976±12	519±79	974±5	800±16
TD3	863±29	965±22	367±113	972±5	683±69
SAC	871±23	971±22	202±50	976±3	746±42
RND	841±35	960±24	385±66	975±3	606±110
SUNRISE	703±26	920±40	285±46	969±4	553±54

environments, obtaining consistent results. The results for other environments can be found in the Appendix C.

RQ3: How the discrepancy of sub-policies impact TEEN’s performance? In order to validate the benefits of trajectory-aware exploration, we conduct experiments in the Ant-v3 environment, progressively increasing the weight parameter denoted as α . We adjust the value of the weight α from $[0, 0.2, 0.5, 1]$. With $\alpha = 0$, we show the performance without trajectory-aware exploration. As the results presented in Figure 3, with adequate reward scale, TEEN improves the performance with the use of trajectory-aware exploration. The effectiveness of the approach fluctuates with changes in reward scale. For a large α value, TEEN aims to enhance the diversity of trajectories. However, as α increases, TEEN fails to effectively utilize reward signals, resulting in sub-optimal performance. In the experiment, we used $\alpha = 0.2$ for the MuJoCo control suites. However, the reward scales in the DeepMind control suites are significantly smaller than those in the MuJoCo control suites. In the MuJoCo control suite, the accumulated reward exceeds 5,000 in the Ant environment, while in the DeepMind control suite, the maximum accumulated reward for all tasks is 1,000. As a result, we utilized a smaller $\alpha = 0.02$ for the DeepMind control suite, considering the smaller reward scale. We also conducted ablation studies with varying reward scales across different environments, please refer to Appendix C for more details.

7 Conclusion

This paper presents a theoretical analysis of the ensemble policy’s diversity exploration problem, based on trajectory distribution. We innovatively discover that the diversity of the ensemble policy can only be enhanced by increasing the Kullback-Leibler (KL) divergence of the sub-policies when entropy is used as the measure of diversity. Guided by this analysis, we introduce the Trajectories-aware Ensemble Exploration (TEEN) method — a novel approach that encourages diverse exploration by improving the diversity of trajectories. Our experiments demonstrate that TEEN consistently elevates the performance of existing off-policy RL algorithms such as TD3, SAC, RND, and ensemble RL algorithms like SUNRISE. There are still important issues to be resolved, e.g., TEEN is sensitive to the reward scale resulting in poor performance without a proper parameter setting. We hope these will be addressed by the community in the future.

Acknowledgments

This work was funded by the National Key R&D Program of China (2021YFC2800500).

References

- [1] Sutton, R. S., A. G. Barto. *Reinforcement learning: An introduction*. MIT press, 2018.
- [2] Mnih, V., K. Kavukcuoglu, D. Silver, et al. Human-level control through deep reinforcement learning. *nature*, 518(7540):529–533, 2015.
- [3] Mnih, V., A. P. Badia, M. Mirza, et al. Asynchronous methods for deep reinforcement learning. In *International conference on machine learning*, vol. 48 of *JMLR Workshop and Conference Proceedings*, pages 1928–1937. PMLR, 2016.
- [4] Gong, C., Y. Bai, X. Hou, et al. Stable training of bellman error in reinforcement learning. In *Neural Information Processing: 27th International Conference, ICONIP 2020, Bangkok, Thailand, November 18–22, 2020, Proceedings, Part V 27*, pages 439–448. Springer, 2020.
- [5] Ye, Y., X. Zhang, J. Sun. Automated vehicle’s behavior decision making using deep reinforcement learning and high-fidelity simulation environment. *Transportation Research Part C: Emerging Technologies*, 107:155–170, 2019.
- [6] Gong, C., Z. Yang, Y. Bai, et al. Mind your data! hiding backdoors in offline reinforcement learning datasets. *arXiv preprint arXiv:2210.04688*, 2022.
- [7] Andrychowicz, M., F. Wolski, A. Ray, et al. Hindsight experience replay. In *Advances in Neural Information Processing Systems*, vol. 30. Curran Associates, Inc., 2017.
- [8] Lillicrap, T. P., J. J. Hunt, A. Pritzel, et al. Continuous control with deep reinforcement learning. In *4th International Conference on Learning Representations, ICLR 2016, San Juan, Puerto Rico, May 2-4, 2016, Conference Track Proceedings*. 2016.
- [9] Silver, D., T. Hubert, J. Schrittwieser, et al. A general reinforcement learning algorithm that masters chess, shogi, and go through self-play. *Science*, 362(6419):1140–1144, 2018.
- [10] Silver, D., J. Schrittwieser, K. Simonyan, et al. Mastering the game of go without human knowledge. *Nature*, 550(7676):354–359, 2017.
- [11] Lan, Q., Y. Pan, A. Fyshe, et al. Maxmin q-learning: Controlling the estimation bias of q-learning. In *8th International Conference on Learning Representations, ICLR 2020, Addis Ababa, Ethiopia, April 26-30, 2020*. OpenReview.net, 2020.
- [12] He, Q., X. Hou. WD3: taming the estimation bias in deep reinforcement learning. In *32nd IEEE International Conference on Tools with Artificial Intelligence, ICTAI 2020, Baltimore, MD, USA, November 9-11, 2020*, pages 391–398. IEEE, 2020.
- [13] He, Q., T. Zhou, M. Fang, et al. Eigensubspace of temporal-difference dynamics and how it improves value approximation in reinforcement learning. In *Joint European Conference on Machine Learning and Knowledge Discovery in Databases*, vol. 14172 of *Lecture Notes in Computer Science*, pages 573–589. Springer, 2023.
- [14] Fujimoto, S., H. Hoof, D. Meger. Addressing function approximation error in actor-critic methods. In *Proceedings of the 35th International Conference on Machine Learning, ICML 2018*, vol. 80 of *Proceedings of Machine Learning Research*, pages 1582–1591. PMLR, PMLR, 2018.
- [15] Osband, I., C. Blundell, A. Pritzel, et al. Deep exploration via bootstrapped dqn. In *Proceedings of the 30th International Conference on Neural Information Processing Systems*, NIPS’16, page 4033–4041. Curran Associates Inc., 2016.
- [16] Lee, K., M. Laskin, A. Srinivas, et al. Sunrise: A simple unified framework for ensemble learning in deep reinforcement learning. In *International Conference on Machine Learning*, pages 6131–6141. PMLR, 2021.
- [17] Chen, X., C. Wang, Z. Zhou, et al. Randomized ensembled double q-learning: Learning fast without a model. In *9th International Conference on Learning Representations, ICLR 2021, Virtual Event, Austria, May 3-7, 2021*. OpenReview.net, 2021.

[18] Hasselt, H. v., A. Guez, D. Silver. Deep reinforcement learning with double q-learning. In *Proceedings of the Thirtieth AAAI Conference on Artificial Intelligence, AAAI'16*, page 2094–2100. AAAI Press, 2016.

[19] Hasselt, H. Double q-learning. In *Advances in Neural Information Processing Systems*, vol. 23. Curran Associates, Inc., 2010.

[20] He, Q., H. Su, J. Zhang, et al. Frustratingly easy regularization on representation can boost deep reinforcement learning. In *IEEE/CVF Conference on Computer Vision and Pattern Recognition, CVPR 2023, Vancouver, BC, Canada, June 17-24, 2023*, pages 20215–20225. IEEE, 2023.

[21] Zahavy, T., Y. Schroecker, F. Behbahani, et al. Discovering policies with domino: Diversity optimization maintaining near optimality. *arXiv preprint arXiv:2205.13521*, 2022.

[22] Haarnoja, T., A. Zhou, P. Abbeel, et al. Soft actor-critic: Off-policy maximum entropy deep reinforcement learning with a stochastic actor. In *Proceedings of the 35th International Conference on Machine Learning, ICML 2018*, vol. 80 of *Proceedings of Machine Learning Research*, pages 1856–1865. PMLR, PMLR, 2018.

[23] Pathak, D., P. Agrawal, A. A. Efros, et al. Curiosity-driven exploration by self-supervised prediction. In *Proceedings of the 34th International Conference on Machine Learning*, vol. 70 of *Proceedings of Machine Learning Research*, pages 2778–2787. PMLR, 2017.

[24] Burda, Y., H. Edwards, A. J. Storkey, et al. Exploration by random network distillation. In *7th International Conference on Learning Representations, ICLR 2019, New Orleans, LA, USA, May 6-9, 2019*. OpenReview.net, 2019.

[25] Todorov, E., T. Erez, Y. Tassa. Mujoco: A physics engine for model-based control. In *2012 IEEE/RSJ International Conference on Intelligent Robots and Systems*, pages 5026–5033. 2012.

[26] Tassa, Y., Y. Doron, A. Muldal, et al. Deepmind control suite. *arXiv preprint arXiv:1801.00690*, 2018.

[27] Wu, D., X. Dong, J. Shen, et al. Reducing estimation bias via triplet-average deep deterministic policy gradient. *IEEE Transactions on Neural Networks and Learning Systems*, 31(11):4933–4945, 2020.

[28] Wei, W., Y. Zhang, J. Liang, et al. Controlling underestimation bias in reinforcement learning via quasi-median operation. *Proceedings of the AAAI Conference on Artificial Intelligence*, 36(8):8621–8628, 2022.

[29] Silver, D., G. Lever, N. Heess, et al. Deterministic policy gradient algorithms. In *Proceedings of the 31st International Conference on International Conference on Machine Learning - Volume 32*, ICML'14, page I-387–I-395. JMLR.org, 2014.

[30] Faußer, S., F. Schwenker. Neural network ensembles in reinforcement learning. *Neural Processing Letters*, 41:55–69, 2015.

[31] Wu, S., J. Yao, H. Fu, et al. Quality-similar diversity via population based reinforcement learning. In *The Eleventh International Conference on Learning Representations, ICLR 2023, Kigali, Rwanda, May 1-5, 2023*. OpenReview.net, 2023.

[32] Eysenbach, B., A. Gupta, J. Ibarz, et al. Diversity is all you need: Learning skills without a reward function. In *7th International Conference on Learning Representations, ICLR 2019*. OpenReview.net, 2019.

[33] Laskin, M., H. Liu, X. B. Peng, et al. Unsupervised reinforcement learning with contrastive intrinsic control. In *Advances in Neural Information Processing Systems*, vol. 35, pages 34478–34491. Curran Associates, Inc., 2022.

[34] Sharma, A., S. Gu, S. Levine, et al. Dynamics-aware unsupervised discovery of skills. In *8th International Conference on Learning Representations, ICLR 2020*. OpenReview.net, 2020.

[35] Jiang, Z., J. Gao, J. Chen. Unsupervised skill discovery via recurrent skill training. In *Advances in Neural Information Processing Systems*, vol. 35, pages 39034–39046. Curran Associates, Inc., 2022.

[36] Kumar, S., A. Kumar, S. Levine, et al. One solution is not all you need: Few-shot extrapolation via structured maxent rl. *Advances in Neural Information Processing Systems*, 33:8198–8210, 2020.

[37] Zhou, Z., W. Fu, B. Zhang, et al. Continuously discovering novel strategies via reward-switching policy optimization. *arXiv preprint arXiv:2204.02246*, 2022.

[38] Sun, H., Z. Peng, B. Dai, et al. Novel policy seeking with constrained optimization. *arXiv preprint arXiv:2005.10696*, 2020.

[39] Masood, M., F. Doshi-Velez. Diversity-inducing policy gradient: Using maximum mean discrepancy to find a set of diverse policies. In *Proceedings of the Twenty-Eighth International Joint Conference on Artificial Intelligence, IJCAI-19*, pages 5923–5929. International Joint Conferences on Artificial Intelligence Organization, 2019.

[40] Fontaine, M., S. Nikolaidis. Differentiable quality diversity. In *Advances in Neural Information Processing Systems*, vol. 34, pages 10040–10052. Curran Associates, Inc., 2021.

[41] Parker-Holder, J., A. Pacchiano, K. M. Choromanski, et al. Effective diversity in population based reinforcement learning. *Advances in Neural Information Processing Systems*, 33:18050–18062, 2020.

[42] Li, C., C. Gong, Q. He, et al. Centralized cooperative exploration policy for continuous control tasks. In *Proceedings of the 2023 International Conference on Autonomous Agents and Multiagent Systems*, pages 2454–2456. 2023.

[43] Haarnoja, T., H. Tang, P. Abbeel, et al. Reinforcement learning with deep energy-based policies. In *Proceedings of the 34th International Conference on Machine Learning*, vol. 70 of *ICML’17*, page 1352–1361. JMLR.org, 2017.

[44] Gong, C., Z. Yang, Y. Bai, et al. Curiosity-driven and victim-aware adversarial policies. In *Proceedings of the 38th Annual Computer Security Applications Conference, ACSAC ’22*, page 186–200. Association for Computing Machinery, 2022.

[45] Silver, D., G. Lever, N. Heess, et al. Deterministic policy gradient algorithms. In *Proceedings of the 31st International Conference on International Conference on Machine Learning - Volume 32*, ICML’14, page I-387–I-395. JMLR.org, 2014.

[46] Sutton, R. S. Learning to predict by the methods of temporal differences. *Machine Learning*, 3(1):9–44, 1988.

[47] Bellman, R. Dynamic programming. *Science*, 153(3731):34–37, 1966.

[48] Kuznetsov, A., P. Shvchikov, A. Grishin, et al. Controlling overestimation bias with truncated mixture of continuous distributional quantile critics. In *the International Conference on Machine Learning (ICML)*, pages 5556–5566. PMLR, 2020.

[49] Liu, H., P. Abbeel. Aps: Active pretraining with successor features. In *International Conference on Machine Learning*, pages 6736–6747. PMLR, 2021.

[50] Anschel, O., N. Baram, N. Shimkin. Averaged-dqn: Variance reduction and stabilization for deep reinforcement learning. In *International conference on machine learning*, pages 176–185. PMLR, 2017.

[51] Zhao, Y., Q. Ye, W. Wu, et al. Generative prompt model for weakly supervised object localization. In *Proceedings of the IEEE/CVF International Conference on Computer Vision (ICCV)*, pages 6351–6361. 2023.

[52] Kingma, D. P., J. Ba. Adam: A method for stochastic optimization. In *ICLR (Poster)*. 2015.

[53] Wang, Y., K. Dong, X. Chen, et al. Q-learning with ucb exploration is sample efficient for infinite-horizon mdp. In *International Conference on Learning Representations*.

[54] David, H. A., H. N. Nagaraja. *Order statistics*. John Wiley & Sons, 2004.

A Theoretical Derivations

Lemma 1 (Ensemble Sample Diversity Decomposition) Given the state-action visit distribution of the ensemble policy ρ . The entropy of this distribution is $\mathcal{H}(\rho)$. Notice that this term can be decomposed into two parts:

$$\mathcal{H}(\rho) = \mathbb{E}_z [\mathcal{D}_{\mathcal{KL}}(\rho(s, a|z_k) || \rho(s, a))] + \mathcal{H}(\rho|z) \quad (1)$$

Proof.

$$\begin{aligned} \mathcal{H}(\rho) &= \mathbb{E}_{(s,a) \sim \rho} [-\log(\rho(s, a))] \\ &= \mathbb{E}_{(s,a,z) \sim \rho} \left[\log \frac{\rho(s, a|z)}{\rho(s, a)} - \log \rho(s, a|z) \right] \\ &= \mathbb{E}_z [\mathcal{D}_{\mathcal{KL}}(\rho(s, a|z) || \rho(s, a))] + \mathcal{H}(\rho|z) \end{aligned} \quad (2)$$

□

Lemma 2 (Equivalent optimization target)

$$H(z|\rho) \propto -\mathcal{D}_{\mathcal{KL}} \left[\rho(s, a|z) || \frac{1}{n} \sum_{k=1}^n \rho(s, a|z_k) \right] \quad (3)$$

Proof. By definition,

$$I(\rho; z) = H(\rho) - H(\rho|z) = H(z) - H(z|\rho) \quad (4)$$

By randomly selecting the latent variable z , we consider that $H(z)$ is a constant depending on the number of z . Thus, we have,

$$\begin{aligned} H(z|\rho) &= H(z) + H(\rho|z) - H(\rho) \\ &\propto \mathbb{E}_{(s,a,z) \sim \rho(s,a,z)} [-\log \rho(s, a|z)] - \mathbb{E}_{(s,a) \sim \rho(s,a)} [-\log \rho(s, a)] \\ &= \mathbb{E}_{(s,a,z) \sim \rho(s,a,z)} [-\log \rho(s, a|z)] - \int -\rho(s, a) \log \rho(s, a) dsda \\ &= \mathbb{E}_{(s,a,z) \sim \rho(s,a,z)} [-\log \rho(s, a|z)] - \int -\rho(s, a, z) \log \rho(s, a) dsdadz \\ &= \mathbb{E}_{(s,a,z) \sim \rho(s,a,z)} [\log \rho(s, a) - \log \rho(s, a|z)] \end{aligned} \quad (5)$$

Where, $\rho(s, a) = \int \rho(s, a|z)p(z)dz = \frac{1}{n} \sum_{k=1}^n \rho(s, a|z_k)$.
Then,

$$\begin{aligned} H(z|\rho) &= \mathbb{E}_{(s,a,z) \sim \rho(s,a,z)} [-\log \rho(z|s, a)] \\ &= H(z) + H(\rho|z) - H(\rho) \\ &\propto \mathbb{E}_{(s,a,z) \sim \rho(s,a,z)} \left[\frac{1}{n} \sum_{k=1}^n \rho(s, a|z_k) - \log \rho(s, a|z) \right] \\ &\propto -\mathcal{D}_{\mathcal{KL}} \left[\rho(s, a|z) || \frac{1}{n} \sum_{k=1}^n \rho(s, a|z_k) \right] \end{aligned} \quad (6)$$

□

Lemma 3 Let X_1, X_2, \dots, X_N be an infinite sequence of i.i.d. random variables with a probability density function (PDF) of $f(x)$ and a cumulative distribution function (CDF) of $F(x)$. Let $X_{1:N} \leq X_{2:N} \leq \dots \leq X_{N:N}$ be the order statistics corresponding to $\{X_i\}_N$. Denote PDF and CDF of the k -th order statistic $X_{k:N}$ as $f_{k:N}$ and $F_{k:N}$ respectively. The following statements hold.

(i) $F_{N:N}(x) = (F(x))^N$. $f_{N:N}(x) = Nf(x)(F(x))^{N-1}$

(ii) $F_{1:N}(x) = 1 - (1 - F(x))^N$. $f_{1:N}(x) = Nf(x)(1 - F(x))^{N-1}$

(iii) $\mu - \frac{(N-1)\sigma}{\sqrt{2N-1}} \leq \mathbb{E}[X_{1:N}] \leq \mu, N > 1. \mathbb{E}[X_{1:N+1}] \leq \mathbb{E}[X_{1:N}]$

(iv) Let $\bar{X} = \frac{1}{N} \sum_{i=1}^N X_i$, then, $\mathbb{E}[\bar{X}] = \mu, \text{Var}[\bar{X}] = \frac{1}{N}\sigma^2$

Proof. (i) We start from the CDF of $X_{N:N}$. By definition, $F_{N:N}(x) = P(X_{N:N} \leq x) = P(X_1 \leq x, X_2 \leq x, \dots, X_N \leq x)$. Under the assumption of iid. $P(X_1 \leq x, X_2 \leq x, \dots, X_N \leq x) = P(X_1 \leq x)P(X_2 \leq x) \dots P(X_N \leq x) = (F(x))^N$. The PDF of $X_{N:N}$ can be derived by taking the derivative of PDF. $f_{N:N} = \frac{dF_{N:N}(x)}{dx} = Nf(x)(F(x))^{N-1}$.

(ii) Similar to (i), $F_{1:N}(x) = P(X_{1:N} \leq x) = 1 - P(x \leq X_{1:N}) = P(x \leq X)P(x \leq X_1, x \leq X_2, \dots, x \leq X_N)$. Under the assumption of iid. $P(x \leq X_1, x \leq X_2, \dots, x \leq X_N) = P(X_1 \geq x)P(X_2 \geq x) \dots P(X_N \geq x)$. Satisfying the normalization, we have $P(X_1 \geq x)P(X_2 \geq x) \dots P(X_N \geq x) = (1 - P(X_1 \leq x))(1 - P(X_2 \leq x)) \dots (1 - P(X_N \leq x)) = (1 - F(x))^N$. Thus, $F_{1:N}(x) = 1 - (1 - F(x))^N$. By taking the derivative of PDF, $f_{1:N}(x) = Nf(x)(1 - F(x))^{N-1}$.

(iii) The detailed proof can be found in [54]. An brief proof is provided as follows. By definition,

$$\begin{aligned} \mathbb{E}[X_{1:N}] &= \int_{-\infty}^{+\infty} xf_{1:N}(x)dx \\ &\stackrel{(i)}{=} \int_{-\infty}^{+\infty} xNf(x)(1 - F(x))^{N-1}dx \\ &\stackrel{u=F(x)}{=} \int_0^1 x(u)N(1 - u)^{N-1}du \end{aligned} \quad (7)$$

To obtain the lower bound on $\mathbb{E}[X_{1:N}]$, we consider the extremum of $\mathbb{E}[X_{1:N}]$ and constrains of mean and variance. For simplification, we consider zero-mean distribution with $\mu = 0$ and σ^2 . The lower bound can be obtained by applying Cauchy-Buniakowsky-Schwarz inequality,

$$\left(\int_0^1 x(u)N(1 - u)^{N-1}du \right)^2 \leq \int_0^1 x^2 du \int_0^1 (N(1 - u)^{N-1})^2 du = \frac{(N-1)^2}{2N-1}\sigma^2, N > 1 \quad (8)$$

Thus, we have $\mathbb{E}[X_{1:N}] \geq \mu - \frac{N-1}{\sqrt{2N-1}}\sigma$ for distribution with mean and variance of μ and σ^2 respectively. By definition, $\mathbb{E}[X_{1:N+1}] = \mathbb{E}[\min(X_{1:N}, X_{N+1})] \leq \mathbb{E}[X_{1:N}]$

(iv) By definition,

$$\mathbb{E}[\bar{X}] = \mathbb{E}\left[\frac{1}{N} \sum_{i=1}^N X_i\right] = \frac{1}{N} \sum_{i=1}^N \mathbb{E}[X_i] = \mu \quad (9)$$

$$\begin{aligned} \text{Var}[\bar{X}] &= \text{Var}\left[\frac{1}{N} \sum_{i=1}^N X_i\right] \\ &= \mathbb{E}\left[\left(\frac{1}{N} \sum_{i=1}^N X_i\right)^2\right] - \mathbb{E}^2\left[\frac{1}{N} \sum_{i=1}^N X_i\right] \\ &= \frac{1}{N^2} \mathbb{E}\left[\sum_{i=1}^N \sum_{j=1}^N X_i X_j\right] - \mu^2 \\ &= \frac{1}{N^2} \mathbb{E}\left[\sum_{i=1}^N X_i^2\right] + \frac{1}{N^2} \sum_{i=1}^N \sum_{j=1, j \neq i}^N \mathbb{E}[X_i] \mathbb{E}[X_j] - \mu^2 \\ &= \frac{1}{N}(\mu^2 + \sigma^2) - \frac{1}{N}\mu^2 \\ &= \frac{1}{N}\sigma^2 \end{aligned} \quad (10)$$

□

B Experimental Details

B.1 Experimental Setup

To validate the generalization, we evaluate our proposed algorithm on environments from MuJoCo Control Suite [25] and DMControl Suite [26]. We use the publicly available environments without any modification. We present screenshots in Figure 1.

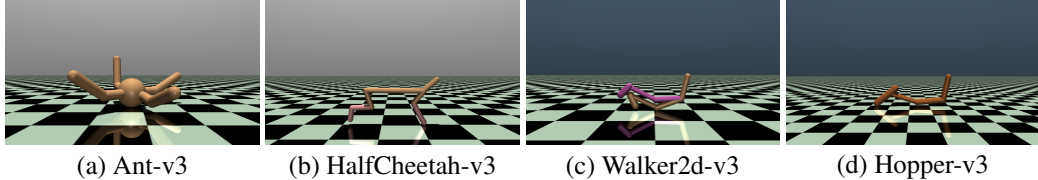


Figure 1: Screenshots of MuJoCo environments.

B.2 Implementation and Hyper-parameters

Here, we describe certain implementation details of TEEN. For our implementation of TEEN, we use a combination of TD3 [14] and TEEN, where we construct N TD3 agents based on the released code by the autor (<https://github.com/sfujim/TD3>). We implement a total of $N = 10$ TD3 agents through out our entire experiments. For recurrent optimization mentioned in section 4.2, we set the period of recurrent training to be 50k. We provide explicit parameters used in our algorithm in Table 1.

B.3 Reproducing Baselines

For reproduction of TD3, we use the official implementation (<https://github.com/sfujim/TD3>). For implementation of SAC, we use the code the author provided and use the parameters the author recommended. We use a single Gaussian distribution and use the environment-dependent reward scaling as described by the authors. For a fair comparison, we apply the version of soft target update and train one iteration per time step.

Table 1: TEEN Parameters settings

Parameter	Value
Exploration policy	$\mathcal{N}(0, 0.1)$
Weight α	0.2
Number of sub-policies N	10
Number of target values M	2
Variance of exploration noise	0.2
Random starting exploration time steps	2.5×10^4
Optimizer	Adam[52]
Learning rate for actor	3×10^{-4}
Learning rate for critic	3×10^{-4}
Replay buffer size	1×10^6
Batch size	256
Discount (γ)	0.99
Number of hidden layers	2
Number of hidden units per layer	256
Activation function	ReLU
Iterations per time step	1
Target smoothing coefficient (η)	5×10^{-3}
Variance of target policy smoothing	0.2
Noise clip range	$[-0.5, 0.5]$
Target critic update interval	2

C Additional Experimental Results

C.1 Additional Evaluation

To convince our evaluation, we conduct our algorithm in a challenging environment Humanoid-v3 in the MuJoCo suite, which is shown in Figure 2. The state dimension of Humaniod is 376, which is exceptionally difficult to solve. We compared our algorithm TEEN with sample-efficient algorithms TD3 and SAC. We follow the standard evaluation settings, carrying out experiments over five million (5e6) steps and running all baselines with 5 random seeds.

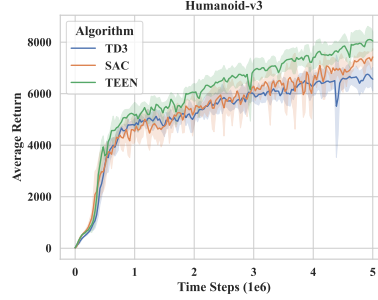


Figure 2: Learning curves for MuJoCo complex task Humanoid-v3. For better visualization, the curves are smoothed uniformly. The bolded line represents the average evaluation over 5 seeds. The shaded region represents a standard deviation of the average evaluation over 5 seeds.

C.2 Additional Ablation Studies

We perform ablation studies on other environments in the MuJoCo suite and show the learning cuives in Figure 3. All the experiments are performed over 5 random seeds with one million (1e6) steps.

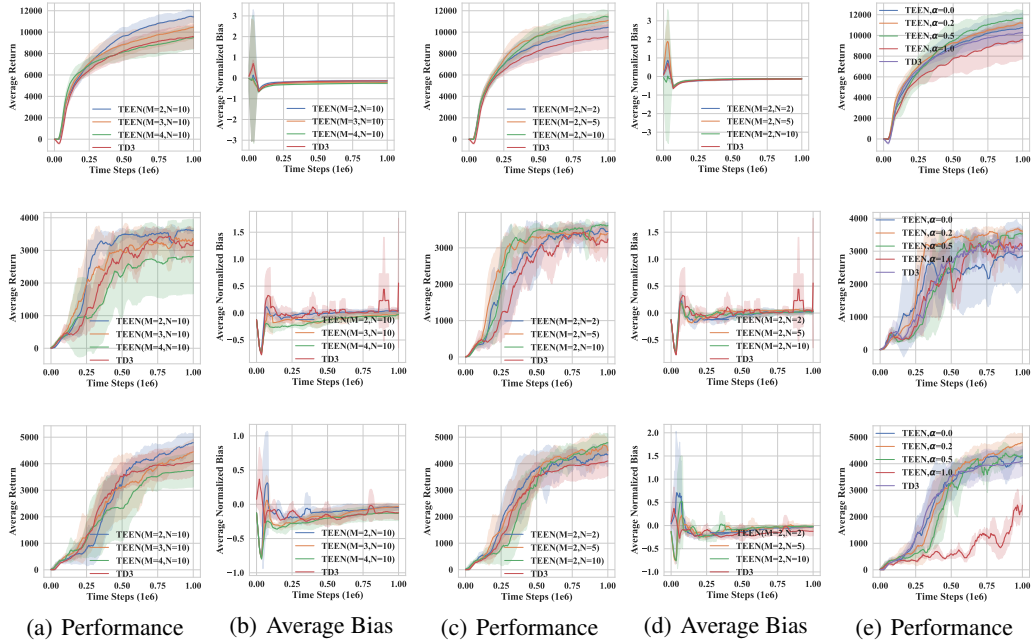


Figure 3: TEEN ablation results for MuJoCo environments (From top to bottom are HalfCheetah-v3, Hopper-v3, Walker2d-v3.). The first column shows the effect of ensemble size N on performance. The second column shows the effect of ensemble size N on estimation bias. The third and fourth columns show the effect of target value number M on both performance and estimation bias respectively. The fifth column shows the effect of weight parameter α on performance.